

54 / 1979

Andrzej Ziabicki

SUPERPOSITION
OF VARIOUS NUCLEATION MECHANISMS
OF THE MORPHOLOGY
OF POLYMER CRYSTALLIZATION

P. 269



WARSZAWA 1979

Praca wpłynęła do Redakcji dnia 25 września 1979 r.

Zarejestrowana pod nr 54/1979



57192



Na prawach rękopisu

Instytut Podstawowych Problemów Techniki PAN

Nakład 140 egz. Ark.wyd. 1,8. Ark.druk. 2 .

Oddano do drukarni w październiku 1979 r.

Nr zamówienia 679/0/79

Warszawska Drukarnia Naukowa, Warszawa,
ul.Śniadeckich 8

Andrzej Ziabicki
Pracownia Fizyki Polimerów
IPPT PAN, Warszawa

SUPERPOSITION OF VARIOUS NUCLEATION MECHANISMS
AND THE MORPHOLOGY OF POLYMER CRYSTALLIZATION

INTRODUCTION

Many attempts have been made to explain the sources of various morphological forms in crystalline polymers. The thermodynamic theories^{1,2} include an implicit assumption that the polymer exists in thermodynamic equilibrium, what is far from reality. The kinetic theories of chain folding³, or bundle-like crystallization⁴ based on specific morphological assumptions describe structures which have been assumed a priori, and therefore do not provide independent predictions. Nevertheless, the kinetic approach, combining thermodynamic driving force and rate effects related to molecular mobility, seems to be the right source of information about the resulting structures. Unfortunately, as shown in our earlier papers⁵ there is no continuous transition from one morphology to another (say, from regular chain folding, to bundle-like crystallization) and one cannot write (and solve) various nucleation and growth processes leading to different morphologies using a single equation with morphology-dependent parameters.

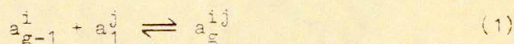
The best way of solving morphological problems seems to be provided by the theory of superposed, or multicomponent nucleation. Fundamentals of the theory of multicomponent growth have been laid by Price⁶, Lauritzen, DiMarzio and Passaglia⁷, DiMarzio⁸ and others⁹; this theory has been used for the discussion of several problems related^{to} the structure of chain-folded crystals^{8,9,10}. The main idea of the multicomponent growth theory in general, and many-mode crystallization in particular, is that crystals are not formed in a "pure" way, i.e. with all elementary units added in exactly the same way, but a superposition of differently arranged units is possible. The appropriate thermodynamic and kinetic factors control the rates with which individual units are attached to a growing cluster (crystal) and, consequently, determine the composition of a mixed crystal. The distribution of different units in such a crystal provides the morphological information required (say, fractions of segments regularly chain-folded, added in a bundle-like fashion, or folded with switchboard reentry). Looking from a theoretical point of view, there is hardly any general reason why the resulting crystal structure (and crystal morphology) should be "pure" rather than "mixed". If, in some special cases such reasons for "pure" morphology do exist - they should be revealed by kinetic considerations.

The application of superposition of various morphologies proposed by the author two years ago^{5,11} will be discussed here and illustrated with a numerical calculation of a simple model involving only three modes of crystal growth: regular chain folding, "switchboard" chain folding and bundle-like addition.

The example shows wide perspectives of the superposition scheme in analyzing systems with competitive ways of crystallization. To obtain numerically significant solutions of crystallization problems, one has to accumulate first information about the thermodynamic (δF_g^{ij}) and kinetic parameters (H^{ij}) appearing in the superposition scheme. Also, more exact, than used in this paper, kinetic equations will be developed for this purpose.

NUCLEATION EQUATIONS AND RATE CONTROLLING PARAMETERS

Consider a cluster composed of $g-1$ elements, the last element being of the i -th type, to which a j -type element is to be attached. The reversible reaction between the cluster a_{g-1}^i and a single element a_j^j



can be discussed in terms of molar fractions D_{g-1}^{ij} , N_g^j , M_g of clusters of size g ending, respectively, with a pair ij , a single segment j , or any terminal structure.

Unlike in our earlier papers on nucleation kinetics⁵, we shall not continualize the variables g , N_g , M_g , S_g , etc. and retain the original discrete structure of all kinetic equations. This formalism suits better the aim of the present paper, though equivalence of the discrete system of recurrence equations for N_g to a single differential equation for continualized distribution, $f(g)$ used in our earlier papers can be easily shown.

The discrete distribution functions (fractions) M_g , N_g^i ,

P_g^{ij} , are related to each other by the normalization conditions:

$$N_g^j = \sum_i P_g^{ij} \quad (2a)$$

$$M_g = \sum_j N_g^j \quad (2b)$$

When desired, higher order distribution functions, $Q_g^{i \dots z}$ can be introduced. If the rate of addition of a unit "j" to a cluster ending with an "i" unit does not depend on the structure of the remaining portion of the mixed cluster, then the net rate of reaction, or the flux, S_g^{ij} , can be written in the form

$$S_g^{ij} = \alpha_{g-1}^{ij} N_{g-1}^i - \beta_{g-1}^{ij} P_g^{ij} \quad (3)$$

and the total flux, $S_g = \sum_{ij} S_g^{ij}$

$$S_g = \sum_i N_{g-1}^i \sum_j \alpha_{g-1}^{ij} - \sum_{ij} \beta_{g-1}^{ij} P_g^{ij} \quad (4)$$

Equations (3) - (4) can be solved for special cases to yield the fraction of "ij" pairs, p^{ij}

$$p^{ij} = S_g^{ij} / S_g \quad (5)$$

or i-type segments, p^i

$$p^i = \sum_j p^{ij} = \sum_j S_g^{ij} / S_g \quad (6)$$

which characterize the morphology of the resulting crystals. General methods of solving such equations have been discussed by Lauritzen, DiMarzio and Passaglia^{7,8}.

The important parameters which should be specified before any solution to multicomponent nucleation is sought are α_g^{ij} and β_g^{ij} , i.e. the frequencies of attachment and dissociation (or reaction rate constants in both directions). The kinetic theory of nucleation as formulated by Turnbull and Fisher¹² and used in earlier papers by the present author⁵ yields:

$$\alpha_{g-1}^{ij} = A C^j H^{ij} \exp(-z \delta F_g^{ij}/kT) \quad (7)$$

$$\beta_g^{ij} = A \exp[(z-1) \delta F_g^{ij}/kT] \quad (8)$$

where C^j is the fraction of the j -th type of single elements attached to the growing cluster, A is a frequency of molecular motions, independent of cluster size, g , or the type of the reacting elements (i, j); H^{ij} denotes dimensionless reorientation factor, defined as the ratio of the average attachment time, t_o^{ij} , to the total time of entrapment including reorientation time Δt^{ij} (cf.¹³)

$$H^{ij} = \frac{t_o^{ij}}{t_o^{ij} + \Delta t^{ij}} \quad (9)$$

H^{ij} plays an important role in polymer crystallization, leading to the very high sensitivity of crystallization to mole-

cular orientation in the system.

$$\delta F_g^{ij} = \Delta F_g^{ij} - \Delta F_{g-1}^i \quad (10)$$

is the increment of the free energy of the system on the attachment of one element "j" to a g-1 cluster ending with an element "i". z is a numerical partition factor ($z \in 0, 1$).

In the conditions of thermodynamic equilibrium, all fluxes S_g^{ij} vanish. For $S_g^{ij} = 0$, eq.(3) yields the equilibrium distribution

$$(P_g^{ij}/N_g^i)_{eq} = \alpha_{g-1}^{ij}/\beta_g^{ij} \quad (11)$$

The ratio α/β serves thus as equilibrium constant. Substitution of (7) and (8) into (11) yields

$$C^j N_{g-1}^i / P_g^{ij} = (1/H^{ij}) \exp(\delta F_g^{ij}/kT) \quad (12)$$

which looks like standard formula for chemical equilibrium with δF_g^{ij} as free energy of the reaction eq.(1) but for the reorientation factor H^{ij} . One should realize however, that for equilibrium conditions ($S_g^{ij} = 0$) the average time of attachment, t_0^{ij} is infinite, and consequently,

$$H_{eq}^{ij} = 1 \quad (13)$$

and the standard expression for thermodynamic equilibrium is recovered

$$(C^j N_{g-1}^i / P_g^{ij})_{eq} = \exp(\delta F_g^{ij} / kT) \quad (14)$$

After simple rearrangements the equilibrium distributions result in the form:

$$P_g^{ij} = N_{g-1}^i C^j \exp(-\delta F_g^{ij} / kT) \quad (15)$$

$$N_g^i = C^i \prod_{k=2}^g \sum_j C^j \exp(-\delta F_k^{ij} / kT) \quad (16)$$

$$M_g = \sum_i C^i \prod_{k=2}^g \sum_j C^j \exp(-\delta F_k^{ij} / kT) \quad (17)$$

The above (equilibrium) distributions do not characterize the actual morphology resulting in a kinetic process. They are controlled by thermodynamic factors alone (concentrations, C^i , and free energy of attachment, δF_g^{ij}) and do not include the reorientation factor H^{ij} .

The solution of the original kinetic equations (3) - (4) along the lines suggested by Lauritzen, DiMarzio and Passaglia⁷ will be attempted in future papers. For the present, qualitative analysis we will consider a more primitive model.

First, it will be assumed that the free energy of attachment a j -type unit to a cluster ending with an i -th unit does not depend on the nature of the element "i". Consequently, α_g^{ij} and β_g^{ij} reduce to α_g^j and β_g^j , respectively, and the flux to be discussed is S_g^j , rather than S_g^{ij}

$$S_g^j = \alpha_{g-1}^j M_{g-1} - \beta_g^j N_g^j \quad (18)$$

Furthermore, the second (reverse) term in the flux will be assumed small compared to the first (production) one, and neglected

$$S_g^j \approx \alpha_{g-1}^j M_{g-1} ; S_g = \sum_j S_g^j \approx M_{g-1} \sum_j \alpha_{g-1}^j \quad (19)$$

The latter assumption is justified when undercooling is large, and the system is far from thermodynamic equilibrium. Now the fluxes, and the resulting cluster structure depend only on the frequency of production, α_g^j , not on the rate of dissociation, β_g^j . The fraction of clusters of size g , ending with a segment "j" will be

$$p_g^j = N_g^j / M_g = S_g^j / S_g = \alpha_{g-1}^j / \sum_j \alpha_{g-1}^j \quad (20)$$

This ratio is a function of g , i.e. changes with the size of the cluster. The average fraction of j -type elements within a cluster of size g is thus

$$\langle p_g^j \rangle = \frac{g}{\sum_{k=2}^g} (\alpha_{k-1}^j / \sum_j \alpha_{k-1}^j) / (g-1) \quad (21)$$

This simple formula will be used in the numerical example discussed at the end of this paper.

THE EFFECTS OF CRYSTALLIZATION MORPHOLOGY ON THE KINETIC PARAMETERS

The three material characteristics, C^j , H^{ij} , and δF_g^{ij} appearing in the kinetic parameters α_g^{ij} and β_g^{ij} can assume different values for various morphologies thus preferring some morphological forms and discriminating others. We shall discuss these characteristics separately.

The effective concentration of single elements, C^j depends, first of all, on whether crystallization is intramolecular, cooperative, or intermolecular. If many kinetically independent molecules participate in cluster growth, and the distribution of segments to be attached to the clusters (crystals) is uniform in space, C^j reduces to the volume fraction of polymer segments in the system, v_2

$$C^j = v_2 \quad (22)$$

This happens when aggregation of rigid molecules, or liquid-crystal type materials is considered (also viruses, some proteins, etc. Fig. 1a). Another example is provided by lateral growth of bundle-like crystals; the longitudinal growth of such crystals (chain extension) behaves differently (fig. 1b). When, on the other hand, a cooperative, intramolecular process is considered, the effective concentration is always equal to unity

$$C^j = 1 \quad (23)$$

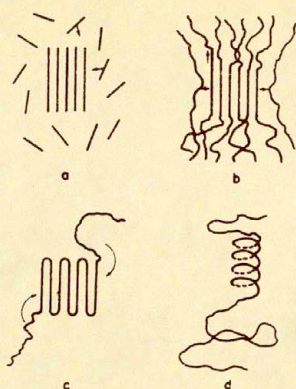


Fig.1. Different morphological forms in polymer crystallization. a. growth from isolated rigid rods; b. bundle-like growth; c. regular chain-folding; d. coil - helix transition.

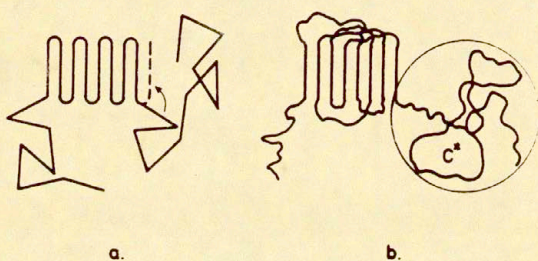


Fig.2. Two types of chain-folded growth: a. regular chain folding with adjacent reentry, b. irregular folding (switchboard structure).

independently of the average volume fraction of the material in the system. This effect has been discussed earlier⁵ and in the polymer field can be well illustrated by regular chain folding (fig.1c), or coil-helix transition (fig.1d). Also longitudinal growth of bundle-like crystals (fig.1b) is cooperative. In a non-cooperative process (eq.22) the probability of addition of each new element to the growing cluster is proportional to the probability of finding a new single element in the surroundings of the cluster, i.e. the volume fraction v_2 . A characteristic feature of a cooperative process is that the elements to be added to the cluster (consecutive segments in the long chain) are provided automatically by the chain, and the probability C is identically equal to unity.

The differentiation between cooperative and non-cooperative polymer crystallization made explicit in our theory⁵ can be observed in several specific nucleation theories concerned with different morphologies. Volume fraction of the polymer, v_2 , appears in the theories of Flory and Mandelkern (cf.¹⁴) who treat always intermolecular, bundle-like crystallization. On the other hand, v_2 does not appear (and it should not) in the theories assuming regular chain folding^{3,9,10}. Polymer concentration does not appear explicitly in the theory of extended chain (bundle-like) crystallization of Calvert and Uhlmann⁴, but it is due, apparently, to the fact that the authors discuss crystallization of melts ($v_2=1$) rather than solutions. Otherwise, eq.(22) should apply.

In the field of polymer crystallization one can distinguish a third possibility, different from both eq.(22) and

eq.(23). It is an intramolecular, but non-cooperative process, when different segments, all coming from one polymer coil are attached irregularly to the growing cluster. The resulting structure, discussed by many polymer morphologists is known as "chain folding with non-adjacent reentry", or "switchboard" structure. Fig.2. illustrates the difference between the regular chain folding (cooperative) and non-cooperative, "switchboard" structure. The process is controlled by the effective concentration of segments within a single polymer coil, C^*

$$C^j = C^* \quad (24)$$

C^* is not equal to the average concentration of polymer in the system, v_2 , and in first approximation is independent of it. On the other hand, C^* is sensitive to the molecular weight of the polymer, chain stiffness (length of the Kuhn segment, a), and polymer-solvent interactions leading to the shrinkage, or swelling of the polymer coil. Using Gaussian approximation for the density distribution around the center of gravity of a polymer coil

$$\rho(r) = N (3/2 \pi \langle R^2 \rangle)^{3/2} \exp(-3r^2/2\langle R^2 \rangle) \quad (25)$$

and the relation for the radius of gyration, $\langle R^2 \rangle$

$$\langle R^2 \rangle = \alpha^2 \langle h^2 \rangle / 6 = \alpha^2 N a^2 / 6 \quad (26)$$

where α is swelling ratio, $\langle h^2 \rangle$ unperturbed (theta) square end-to-end distance, N - number of statistical chain segments in

the chain; and a - length of the chain segment. Integrating eq.(25) one arrives at the average volume fraction of polymer segments in the coil, C^*

$$C^* = (3v_0/4\pi\langle R^2 \rangle)^{3/2} \int_0^R q(r) 4\pi r^2 dr = Nv_0(3/2\pi\langle R^2 \rangle)^{3/2} \times \\ \times [\sqrt{\pi/6} \operatorname{erf}(\sqrt{3/2}) - \exp(-3/2)] = 0.440221 Nv_0(3/2\pi\langle R^2 \rangle)^{3/2} \quad (27)$$

Substituting eq.(26) for $\langle R^2 \rangle$ one obtains

$$C^* = 2.134566 v_0/N^{1/2} a^3 \alpha^3 \quad (28)$$

v_0 is volume of a single chain segment, and $\operatorname{erf}(x)$ is integral error function. The local concentration within a polymer coil decreases with the number of chain segments (molecular weight) faster than $N^{-1/2}$ because the swelling ratio α increases with N . In good solvents (strong swelling, high α) the local concentration will be more reduced.

The significance of the local concentration within macromolecular coil, C^* , for crystallization of polymers from dilute solutions was recognized by Kawai^{15,16}. Kawai suggested that the average volume fraction of polymer, v_2 , appearing in the Flory-Mandelkern theory (for bundle-like morphology) should be replaced by the local concentration, C^* , which is independent of v_2 , but sensitive to (decreasing) molecular weight. Kawai suggested that this can explain the observed independence of fold length in chain-folded crystals on polymer concentration v_2 , and reduction of the X-ray long identity period with in-

creasing molecular weight of polymer¹⁶. This interpretation does not seem to be correct, though. C^* is relevant only for irregular chain folding (switchboard structure) which does not seem to dominate in solution-grown crystals. For regular (cooperative) chain folding C^j should be always unity, also independently of v_2 . The molecular weight dependence can be explained by an other kinetic factor, H^{ij} , to be discussed below.

The reorientation factor, H , (cf. eq. 9) has been introduced to the theory of nucleation a few years ago^{5, 13, 17}. Since H characterizes molecular motions required for effective attachment of a single element to the growing cluster, it is very sensitive to the size, deformability and shape of single elements.

For spherical, or small, nearly spherical single elements molecular rotation ceases to be a necessary step of attachment and, consequently, H becomes a unity

$$\Delta t^{ij}/t_0^{ij} \rightarrow 0 \Rightarrow H^{ij} \rightarrow 1 \quad (29)$$

This is also the case for very slow nucleation processes, close to thermodynamic equilibrium, when $t_0^{ij} \rightarrow \infty$. For rigid, rodlike particles, like viruses, liquid crystals etc. (fig. 1a), H^{ij} is controlled by rotational diffusion constant D_r which decreases with increasing volume of the particle, v_0 , and strongly decreases with increasing asymmetry (aspect ratio) of the particle, p

$$H^{ij} = H^{ij} [D_r(v_0, p)] \quad (30)$$

Much more complicated relations are encountered in deformable, long-chain macromolecules which consist of λ^a number of attachable single elements (chain segments) connected by flexible joints. Two features of the behaviour of such chains should be emphasized.

i. there is a significant difference in the symmetry of efficient rotation bringing the element to the orientation consistent with that of the cluster, between non-cooperative and cooperative processes. When isolated single elements (fig. 1a), or randomly chosen chain segments (bundle-like growth, fig. 1b, or switchboard chain-folding, fig. 2b) approach the cluster, they exhibit a two-fold axis symmetry; they can be reoriented by rotation in either of two opposite directions as illustrated in fig. 3a. On the other hand, cooperative chain folding (fig. 1c), or cooperative helix formation (fig. 1d), admit only one-way rotation, the other way leading to ineffective orientations (fig. 3b). Speaking in terms of the disorientation angle, ϕ , i.e. angle between the cluster axis, and axis of the single element, in non-cooperative systems the admissible orientation is $\phi = 0$ or $\phi = \pi$, while for cooperative growth only $\phi = 0$ is admitted. Consequently, the reorientation time Δt^{ij} for non-cooperative systems is smaller, and H^{ij} generally larger than for cooperative addition.

$$1/\Delta t^{ij} = 1/\Delta t^{ij}(\phi_0 \rightarrow 0) + 1/\Delta t^{ij}(\phi_0 \rightarrow \pi) \quad (31)$$

for cooperative systems, and

$$1/\Delta t^{ij} = 1/\Delta t^{ij}(\phi_0 \rightarrow 0) \quad (32)$$

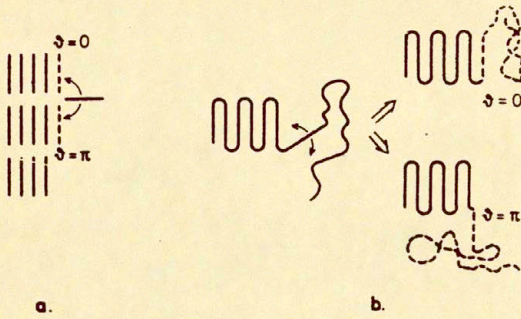


Fig.3. The symmetry of rotation in a: growth from isolated elements, and b: regular chain folding.

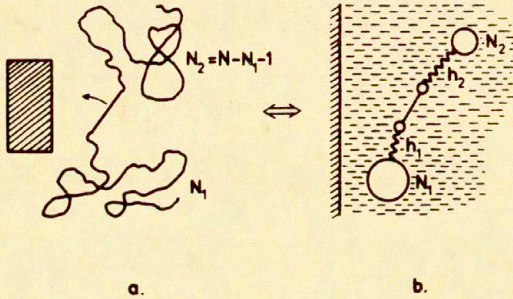


Fig.4. Effects of far segments on the rotation of a single element to be attached to a cluster. a: molecular scheme, b: a rheological model

for non-cooperative, and

$$H_{\text{non-cp}}^{ij} > H_{\text{cp}}^{ij} \quad (33)$$

ii. the other aspect of reorientation of segments in long chains is complex dynamics of cooperative motions and molecular weight dependence. Rotation of one segment, part of a chain composed of N units is associated not only with the hydrodynamic (viscous) drag of the rotation of the segment itself, but also with the viscoelastic response of the two hanging long-chain "tails" with molecular weights N_1 , and $(N-N_1-1)$ times larger than the segment itself. As noted in ref.¹³ rotation in such a system (fig.4 a) can be solved using spring-dashpot models (fig.4 b) and well-known methods of macromolecular hydrodynamics. Two small beads on the ends of the rigid dumbbell (fig.4b) represent viscous drag of the rotating segment, dependent on the size and shape of the segment. Larger beads correspond to (generally different) friction coefficients of the "tails" with molecular weights proportional to N_1 and $(N-N_1-1)$, respectively. Consequently, rotation of the segment depends on the total number of segments in the long chain (N) and on the position of the segment within the chain (N_1/N). For random, non-cooperative attachment one can integrate the rotation velocity (and H^{ij} factors) over the position of the segment along the chain, i.e. from $N_1=1$ to $N_1=N-1$ to obtain average characteristics as functions of the molecular weight (number of statistical chain segments) N . Two asymptotic cases can be mentioned. If the chain is rigid, rotation of the se-

gment to be attached leads to the translation of terminal friction centers. With increasing N (N_1, N_2) the radii h_1, h_2 increase as $N_1^{1/2}, N_2^{1/2}$, and the overall friction forces as $N_1^{3/2}, N_2^{3/2}$. Consequently, the average rotation factor $\langle H^{ij} \rangle$ decreases with increasing molecular weight of the polymer and disappears for very high N

$$\partial \langle H^{ij} \rangle / \partial N < 0; \quad \lim_{N \rightarrow \infty} \langle H^{ij} \rangle = 0 \quad (34)$$

and thus crystallization of smaller (rigid) macromolecules is preferred. Since the resistance to rotation offered by each part of the hanging "tail" increases with N faster than linearly, the minimum resistance (and maximum H^{ij}) corresponds to segments located centrally in the chain ($N_1 = N/2$).

$$(N_1)_{\max} = N/2 \quad (35)$$

On the other hand, when chains are soft and flexible, but translation of chain ends is prohibited by very high viscosity or by crosslinking and stress applied to the system, the resistance experienced by a rotating segment is a combination of the viscous drag of the segment itself, and elastic response of the hanging "tails". The elastic forces being inversely proportional to $N_1, (N-N_1-1)$ we obtain the average rotation factor $\langle H^{ij} \rangle$ which monotonically decreases with increasing N . The limiting value at $N \rightarrow \infty, H_0$, is determined by the viscous drag of the segment itself

$$\partial \langle H^{ij} \rangle / \partial N < 0; \quad \lim_{N \rightarrow \infty} \langle H^{ij} \rangle = H_0 \quad (36)$$

Here again, the optimum position in the chain (maximum H^{ij}) corresponds to the centre, as shown in eq.(35) but longer (flexible) chains are evidently preferred in crystallization to short ones.

The same considerations apply formally to cooperative attachment, but the freedom of choice of the position of the segment in the chain, N_1 , exists only for the first element of the cluster. All other segments, by definition of the cooperative process are determined as N_1+1 , N_1+2 , ..., up to the end of the cooperative sequence. Consequently, differentiation of H^{ij} factors for segments with various positions, N_1 , along the chain and maximum at $N_1 = N/2$ determines the resulting distribution of segments in a non-cooperatively grown cluster, but only a systematic variation of growth rates corresponding to the addition of predetermined consecutive segments in the cooperative case.

In real systems, the behaviour of the rotation factors H^{ij} can be expected to be intermediate between the two asymptotic cases discussed above, as controlled by viscoelastic deformation of polymer chains. With variation of crystallization conditions and materials a wide spectrum of H^{ij} , and a wide range of resulting morphologies can be obtained. The solution of the dynamic problem formulated in¹³ is required for prediction of such variation.

A THREE-COMPONENT EXAMPLE

To illustrate the kind of problems which can be solved using the approach discussed above, we will discuss a simple system allowing for three different morphological modes of growth: regular chain folding ($i=1$), irregular chain folding (switchboard structure, $i=2$), and intermolecular bundle-like addition ($i=3$). Having no detailed information about the respective free energies δF_g^i , we will assume that they are all equal $\delta F_g^1 = \delta F_g^2 = \delta F_g^3$. If crystal lattice structure does not change from one morphology to another, the bulk free energy components of δF_g^i should be all equal. The surface component can be expected to be sensitive to morphology, but its determination would require separate studies. With equal δF_g^i , applying eq.21 we obtain the distribution function p^i , independent of the cluster size g

$$p_g^i = C^i H^i / \sum_{i=1}^3 C^i H^i \quad (37)$$

We will assume further that the rotation factors H^2 and H^3 for both non-cooperative processes are equal to each other and smaller than H^1 for regular chain folding. The effective concentrations for the three processes will be different, viz.

$C^1 = 1$ for the cooperative chain folding

$C^2 = C^* = \text{const.}$ for non-cooperative, intramolecular addition

$C^3 = v_2$ for intermolecular bundle-like growth

where v_2 is volume fraction of polymer in the system, and C^* is the average volume fraction within a single macromolecular coil.

The resulting distribution p^i , i.e. the fractions of segments in the cluster attached according to various modes read :

$$p^1 = P_{\text{chain folding}} = 1/[1 + (H^2/H^1)(C^*+v_2)] \quad (38a)$$

$$p^2 = P_{\text{switchboard}} = (H^2/H^1)C^*/[1 + (H^2/H^1)(C^*+v_2)] \quad (38b)$$

$$p^3 = P_{\text{bundle-like}} = (H^2/H^1)v_2/[1 + (H^2/H^1)(C^*+v_2)] \quad (38c)$$

It can be observed that the content of intramolecular segments (both cooperative, $i=1$ and irregular, $i=2$) is maximum at $v_2 = 0$ and monotonically decreases with increasing polymer concentration, v_2 . The fraction of bundle-like segments, p^3 , starting from zero at $v_2 = 0$ increases with v_2 to some finite value at $v_2 = 1$. The other factor which controls the distribution is the ratio H^2/H^1 . With increasing H^2/H^1 increase fractions of both non-cooperative segments ($i=2$ and $i=3$), while the regularly folded, cooperative segments ($i=1$) become less frequent.

The equilibrium distributions for the above case yield:

$$(p_g^i)_{\text{eq}} = (N_g^i)_{\text{eq}} / (M_g)_{\text{eq}} = C^i \exp(-\delta F_g^i/kT) / \sum_i C^i \exp(-\delta F_g^i/kT) \quad (39)$$

which, with the assumption of equal free energies reduces to the ratio of concentrations, C^i , independent of cluster size, g

$$(p^i)_{\text{eq}} = C^i / \sum_i C^i \quad (39a)$$

In addition to the fractions p_g^i of various segments within the cluster (eqs.38 and 39), two average characteristics can be derived from the above model. The average rate of growth is characterized by the rate constant $\alpha^i = C^i H^i \exp(-z\delta F_g^i/kT)$. In the process of cluster growth these factors are superposed multiplicatively, so the averaging must be performed on logarithms. With the assumption of equal free energies δF_g we will calculate the average preexponential factor defined as

$$\langle CH \rangle = \exp\left[\frac{\sum_i C^i H^i \ln(C^i H^i)}{\sum_i C^i H^i} \right] \quad (40)$$

The other average characteristic related to nucleation is the critical nucleation temperature for the combined, three-component process. As shown in earlier papers⁵ this temperature for a dilute system can be found from the relation

$$T_m/T_m^0 = A/(A - \ln C) \quad (41)$$

where T_m^0 is the critical temperature for an undiluted system ($C=1$) and $A = \Delta h v_o/kT_m^0$.

With equilibrium distribution of segments $(p^i)_{eq}$ from eq.(39a) the average critical temperature $\langle T_m \rangle$ can be approximated by:

$$\langle T_m \rangle / T_m^0 = A/(A - \langle \ln C \rangle) \quad (42)$$

where

$$\langle \ln C \rangle = \frac{\sum_i C^i \ln C^i}{\sum_i C^i} \quad (43)$$

NUMERICAL CALCULATIONS. RESULTS AND DISCUSSION

The fractions p^1 of segments attached according to regular chain folding mechanism ($i=1$), irregular (switchboard-type) folding, $i=2$, and bundle-like mode, $i=3$ were calculated from eqs.(38a-c) for various polymer concentrations, v_2 , and coil densities $C^* = 0.1, 0.01, \text{ and } 0$. The assumed rotation factors for non-cooperative and cooperative processes were $H^2=H^3= 2H^1$. $C^* = 0.1$ seems to be greatly overestimated coil density as corresponding to $N = 20-50$ chain segments in a macromolecule. Figure 5. presents the results. Similar calculations performed for the equilibrium distributions $(p_g^1)_{eq}$ from eq.(39a) are presented in figure 6.

As evident in figure 5. the fraction of regularly folded segments, p^1 , decreases with increasing polymer concentration and that of bundle-like segments, p^3 , behaves in an opposite way. No bundle-like segments exist at zero concentration, $v_2=0$. With increasing coil density, C^* , both p^1 and p^3 are reduced. However, even at unrealistically high $C^* = 0.1$, the fraction of switchboard segments never exceeds 17 % and the switchboard structure does not seem to play any major role. Naturally, in the absence of switchboard segments ($C^* = 0$), at $v_2 = 0$ purely chain-folded crystals are formed, as actually observed in very dilute polymer solutions. With increasing concentration, increasing amounts of bundle-like segments are formed, reaching at $v_2 = 1$ (undiluted polymer) ca 60 %. Unlike at infinite dilution however, in an undiluted system does not result any pure morphology, but always a combination of intra- and intermolecular segments in proportions dependent on the ratio H^2/H^1 and coil

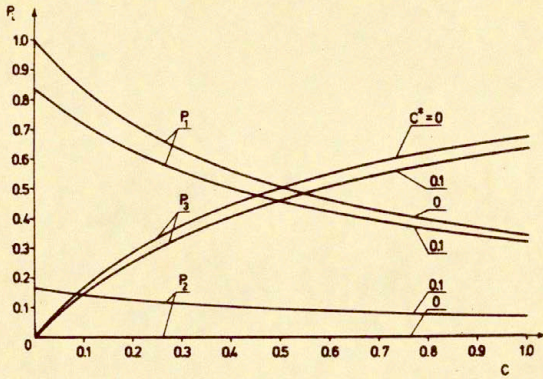


Fig.5. Fractions p_i of chain segments attached according to different growth modes. Kinetic model (eqs.38). $H^2/H^1 = 2$, coil densities, C^* , indicated.

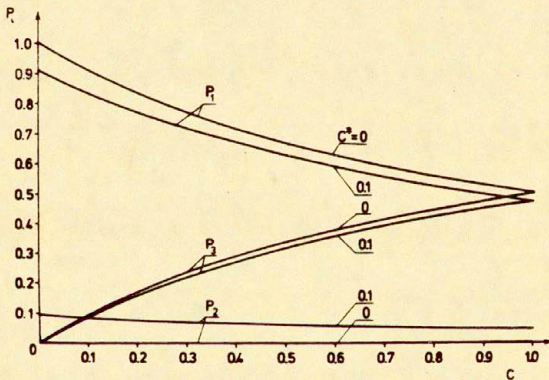


Fig.6. Equilibrium fractions, p_i , of chain segments attached according to different growth modes, as calculated from eq.39a. Coil densities, C^* , indicated.

density C^* .

The equilibrium distributions (figure 6) are similar in shape to the kinetic ones. Being controlled by concentrations alone, the equilibrium fraction of regularly chain-folded segments is generally higher than concentration of bundle-like segments, reaching equal values in the undiluted conditions:

$$p_{eq}^1(v_2=1) = p_{eq}^3(v_2=1) \quad (44)$$

Like in the kinetic case, switchboard structures do not play any important role.

Figure 7. presents the average pre-exponential factor $\langle CH \rangle$ calculated from eq.(40) for $H^1 = 0.5$, $H^2=H^3=1$, various values of v_2 and $C^* = 0.1, 0.01, \text{ and } 0$. The broken horizontal line corresponds to a pure chain-folded mechanism, $CH = 0.5$. It can be observed that in all cases there appears a minimum of $\langle CH \rangle$ in the range of low polymer concentrations ($v_2 = 0.1-0.2$). The minimum is very broad and is slightly shifted towards lower v_2 with increasing C^* ; the depth of the minimum increases with increasing C^* . The $\langle CH \rangle$ vs. v_2 curves are also shifted towards lower $\langle CH \rangle$ values with increasing coil densities C^* . This means that introduction of the possibility of switchboard connection reduces the average growth rate $\langle CH \rangle$. Growth rates above the minimum are controlled by the bundle-like mechanism and increase with the polymer concentration v_2 (and the fraction of bundle-like segments). The average growth rates at higher concentrations are higher than those for pure chain-folding mechanism because of the rotation factor $H^2 > H^1$.

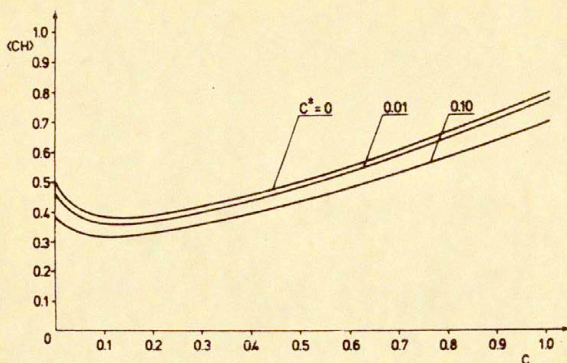


Fig.7. The average kinetic parameter $\langle CH \rangle$ calculated for the kinetic model with $H^1 = 0.5$, $H^2 = H^3 = 1$. Coil densities, C^* , indicated.

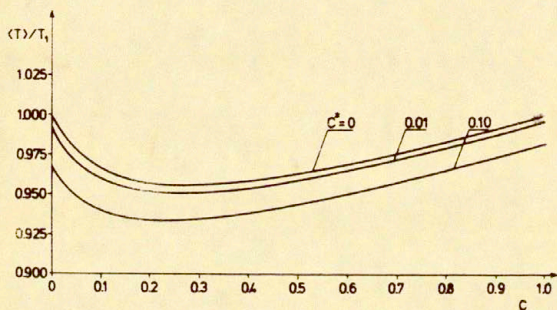


Fig.8. The reduced critical nucleation temperature, $\langle T_m \rangle / T_m^0$ calculated as a function of polymer concentration c . $\Delta h_{21} / k T_m^0 = 6.035$, coil densities, C^* , indicated.

The critical nucleation temperatures $\langle T_m \rangle$ are less sensitive to polymer concentration and morphology than growth rates. As evident in figure 8. the ratio $\langle T_m \rangle / T_m^0$ also exhibits a minimum in the range of small concentrations, the position of which is shifted towards smaller concentrations and whose depth increases with increasing coil density C^* . The minima of $\langle T_m \rangle$ vs. v_2 , and $\langle CH \rangle$ vs. v_2 do not disappear, however, at $C^* = 0$. So, the existence of switchboard segments is not the only source of depression of the critical temperature and of the growth rate. For the examples discussed, critical temperature for mixed crystals in the whole range of polymer concentrations, v_2 , is lower than that for pure chain-folded crystals. Only at $C^* = 0$ (no switchboard segments) can T_m reach the limiting value T_m^0 , viz. when $v_2 = 0$ (pure chain-folded crystals), or $v_2 = 1$ (undiluted system).

CONCLUDING REMARKS

The theory presented in this paper is not complete and so are the numerical examples discussed herein. The simple model discussed above illustrates, however, possibilities offered by the superposed nucleation theory in elucidation of many problems related to structure formation. In spite of many approximations and assumptions used in this paper to compensate for the lack of more reliable information, the main conclusions drawn from the analysis of the three-component model seem to be physically reasonable and qualitatively correct: the secondary importance of switchboard structure, depression of the average

rate of growth and of the critical nucleation temperature in the range of small polymer concentrations, pure chain-folded morphology at infinite dilution ($v_2 \rightarrow 0$) and high molecular weights ($C^* \rightarrow 0$). Quantitatively these predictions may appear to be incorrect when very strong thermodynamic effects exist (very different free energies δF_g^i), or very different reorientation factors H^i apply to various morphologies.

Further research in this field must be concentrated on a more complete solution of the kinetic equations of nucleation (eqs. 3-6) and on the derivation of the absolute values of the reorientation factors H^{ij} and free energies δF_g^{ij} for various morphologies.

ACKNOWLEDGEMENT

This work has been supported in part by the NSP Grant No. INT-76 17522 made available through the Marie Sklodowska - Curie Fund established by contributions of the United States and Polish Governments.

REFERENCES

1. F.C.Frank, Disc.Paraday Soc., 25, 208, (1958)
2. A.Peterlin and E.W.Fischer, Z.Physik 159, 272, (1960)
3. J.I.Lauritzen and J.D.Hoffman, J.Chem.Phys. 31, 1680, (1959);
J.Res.NBS, 64A, 73, (1960)
4. P.D.Calvert and D.R.Uhlmann, J.Appl.Phys., 43, 944, (1972)
5. A.Ziabicki, IFTR Reports No. 60/1977

6. F.P.Price, J.Chem.Phys. 35, 1884, (1961)
7. J.I.Lauritzen, E.A.DiMarzio, and E.Passaglia, J.Chem.Phys. 45, 4444, (1966)
8. E.A.DiMarzio, J.Chem.Phys. 47, 3451, (1967)
9. I.C.Sanchez and E.A.DiMarzio, Macromolecules 4, 677, (1971)
10. I.C.Sanchez, Rev.Macromol.Chem., C10, 113, (1974)
11. A.Ziabicki, Europhysics Conference Abstracts, 2E, 33, (1977)
12. D.Turnbull and J.C.Fisher, J.Chem.Phys., 17, 71, (1949)
13. A.Ziabicki, IFTF Reports, No. 55/1978
14. L.Mandelkern, Crystallization of Polymers, McGraw and Hill, New York, 1963
15. T.Kawai, J.Polymer Sci., B2, 965, (1964)
16. T.Kawai, T.Hama and K.Ehara, Makromol.Chem., 113, 282, (1968)
17. A.Ziabicki, J.Chem.Phys., 66, 1638, (1977)